

The JOINBON SiPM for the readout of LySO crystals: a Multi Voltage Threshold approach

To cite this article: N. D'Ascenzo *et al* 2020 *JINST* **15** C07006

View the [article online](#) for updates and enhancements.



IOP | ebooksTM

Bringing together innovative digital publishing with leading authors from the global scientific community.

Start exploring the collection—download the first chapter of every title for free.

INTERNATIONAL SUMMER SCHOOL ON
INTELLIGENT SIGNAL PROCESSING FOR FRONTIER RESEARCH AND INDUSTRY
HUAZHONG UNIVERSITY OF SCIENCE AND TECHNOLOGY, HUST, AT WUHAN, CHINA
12–26 MAY 2019

The JOINBON SiPM for the readout of LySO crystals: a Multi Voltage Threshold approach

**N. D’Ascenzo,^{a,b,1} L. Wang,^c X. Zhang,^c Q. Lv,^c E. Antonecchia,^{a,b} Y. Lin,^a M. Kattan,^{a,d}
S. Leinweber^{a,d} and Q. Xie^{a,b,1}**

^a*Huazhong University of Science and Technology,
Luoyu Road 1037, Wuhan, China*

^b*IRCCS Neuromed,
Via Atinense 18, 86077 Pozzilli (IS), Italy*

^c*JOINBON Technology Ltd.,
Ezhou, China*

^d*RheinMain University of applied sciences,
Wiesbaden, Germany*

E-mail: ndasc@hust.edu.cn, qgxie@hust.edu.cn

ABSTRACT: The JOINBON Silicon Photomultiplier is a novel commercial silicon sensor for weak photon flux. In this paper we report a characterization of the sensor for the readout of LySO crystals with potential application to Positron Emission Tomography. We measured an energy resolution of approximately $(13.50 \pm 0.03)\%$ (FWHM) and a coincidence time resolution ranging between (215 ± 3) ps for a 5 mm long crystal up to (290 ± 2) ps for a 20 mm long crystal. Finally we tested the feasibility of the JOINBON SiPM to a Multi Voltage Threshold readout and we obtained an energy resolution compatible with the intrinsic system performance.

KEYWORDS: Gamma camera, SPECT, PET PET/CT, coronary CT angiography (CTA); Photon detectors for UV, visible and IR photons (solid-state) (PIN diodes, APDs, Si-PMTs, G-APDs, CCDs, EBCCDs, EMCCDs, CMOS imagers, etc)

¹Corresponding author.

Contents

1	Introduction	1
2	Materials and methods	2
2.1	Silicon photomultipliers	2
2.2	Readout of 3×3 mm ² LySO crystals	2
2.3	Measurement of the saturation response	4
3	Data processing	4
3.1	Energy resolution	4
3.2	Coincidence time resolution	5
3.3	Multi Voltage Threshold scheme	5
4	Results and discussion	6
4.1	Energy resolution	6
4.2	Coincidence time resolution	8
4.3	Multi Voltage Threshold approach	9
5	Conclusion	10

1 Introduction

LySO crystals are commonly used, among others, for radiation detection systems in high energy physics, nuclear medicine and homeland security. Their typical emission wavelength peaks at 420 nm and the average light yield is approximately 26000 optical photons generated in response to a deposited energy of 1 MeV. The Silicon Photomultiplier (SiPM) is nowadays commonly used for the readout of the LySO scintillation light. A stable production of the SiPMs is currently available at few leading manufacturers [1–5]. The commercial SiPM exhibits, among others, a dark count rate as low as 80–100 kHz/mm² [2], a gain up to 6×10^6 at an overvoltage of 2.5 V [2], a photon detection efficiency up to 30%–40% at a wavelength in the range between 400 nm and 420 nm [5], and a single photon time resolution (SPTR) of approximately 100 ps [3].

A key-problem in the development of radiation sensors based on LySO crystals is the design of a proper readout scheme. Digital electronics plays an essential role in the definition of novel readout architectures for radiation detectors. A precise time stamping of a level of few hundreds picoseconds is a basic requirement in order to guarantee a fast response of the detection system. Larger bandwidth and high count-rate per seconds are also beneficial for the collection of a larger statistics, in particular in radiation intensive applications. By way of example novel digital sensor readout electronics configuration with the SiPM allowed to reach a count rate in proton therapy PET monitoring systems ranging between 0.25 Mcps [6] and 3.5 Mcps [7]. Digital sampling-based

electronics has been recently demonstrated to be of vital importance in the improvement of the signal to noise ratio due to the possibility of a better analysis of the sampled detector signals [8–14].

During the past few years we have reported the realization of related high bandwidth digital read-out electronics for radiation sensors [15–30]. As a possible solution to the sampling-rate challenge, we have previously proposed a multi-voltage threshold (MVT) sampling method that takes samples of a pulse with respect to a set of reference voltages. By choosing the reference voltages properly, the MVT method can always obtain samples at the fast leading edge of a pulse. The total energy and the timing of the pulse can be obtained by the digital signal processing of a small set of samples of the pulse. As the pulses are instantaneously digitized and the number of samples per pulse is small, this sampling method can have a high count-rate capability up to 5 Mcps, without requiring a large on-board storage buffer [31–33].

Recently a new SiPM has been announced for commercial distribution by JOINBON Technology Ltd., a company with headquarters in Ezhou, China. The TN1000 and TN3000 SiPM series by JOINBON are developed with a 0.35 μm CMOS process and exhibits, among others, a dark count rate as low as 100 kHz/mm², a gain up to 2.5×10^6 at an overvoltage of 2.5 V, a photon detection efficiency up to 35% at a wavelength in the range between 400 nm and 420 nm and a single photon time resolution (SPTR) of approximately 80 ps [34]. In this paper we report, for the first time to our knowledge, the performance of the readout of the LySO scintillators by means of the TN1050 and TN3050 JOINBON SiPMs, focusing on two potential applications namely positron emission tomography and X-ray scanners for homeland security systems. Furthermore we investigate the possibility of a Multi Voltage Threshold readout in order to simplify the digitalization scheme of the signals.

2 Materials and methods

2.1 Silicon photomultipliers

We used the TN3050 SiPM by JOINBON Ltd, Ezhou, China. It is a $3 \times 3 \text{ mm}^2$ SiPM with 3364 microcells. It is produced with a 0.35 μm CMOS process. A summary of its performances is reported in table 1. The SiPMs were provided in a $4 \times 4 \times 0.68 \text{ mm}^3$ package, as shown in figure 1. We used 20 samples of the TN3050.

2.2 Readout of $3 \times 3 \text{ mm}^2$ LySO crystals

LySO crystals with a transverse size ranging between $2 \times 2 \text{ mm}^2$ and $4 \times 4 \text{ mm}^2$ are commonly used in PET systems [35]. The experimental setup is shown in figure 2. In order to test the performance of the JOINBON SiPM as readout sensor for this nuclear medicine application, two LySO crystals (SANHO OSTOR ELECTRONICS CORP) with a transverse size of $3 \times 3 \text{ mm}^2$ were wrapped with three layers of 0.2 mm thick teflon. One side of each crystal was left uncovered and was coupled with the TN3050 JOINBON SiPM using optical grease. The wrapping and the coupling was repeated before each measurement, in order to avoid the degradation of the light reflection property of the teflon due to the absorption of the optical grease. We measured the impact of the geometry of the scintillators by using crystals with a length of 5 mm, 10 mm, 15 mm and 20 mm.

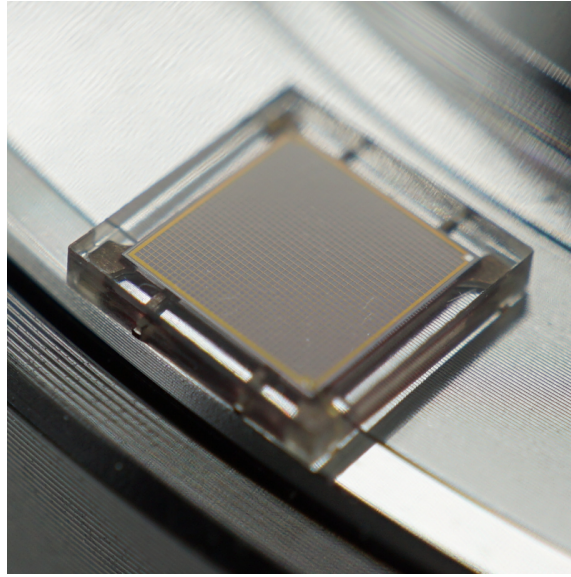


Figure 1. Packaged samples of the TN3050 SiPMs by JOINBON Ltd., Ezhou, China.

Table 1. Technical parameters of the JOINBON TN3050 SiPMs [34]. The technical parameters of the TN1050 series are reported in the table for completeness.

Parameter	TN1050	TN3050
Active area	1 mm ²	9 mm ²
Number of pixels	324	3364
Pitch	50 μm	50 μm
Fill factor	70.6%	70.6%
Peak wavelength	420 nm	420 nm
Breakdown voltage	24.9 V	24.9 V
Overvoltage [V]	1–5 V	1–5 V
Peak PDE at 28 V	35%	35%
Gain at 28 V	3.8×10^6	3.8×10^6
Recovery time	34 ns	45 ns
Rise time	0.9 ns	1.3 ns
Dark count rate at 28 V	120 kHz/mm ²	120 kHz/mm ²
Dark current [nA]	90 nA	714 nA
Temperature coefficient	34.4 mV/K	34.4 mV/K
Cross talk	3.5%	3.5%
Afterpulsing probability	2.0%	2.7%
SPTR at 28 V	80 ps	168 ps

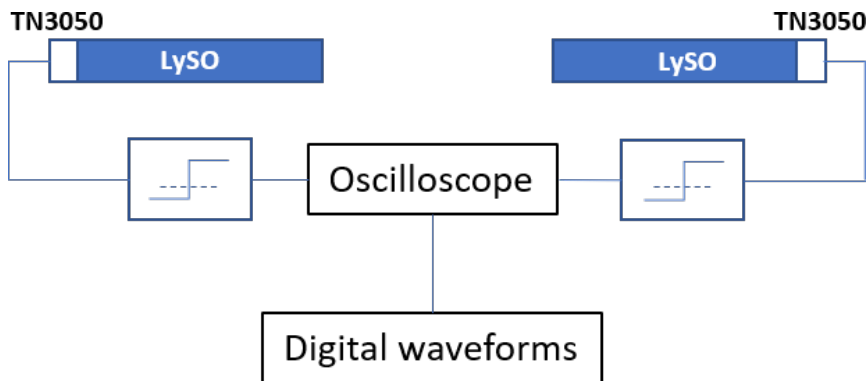


Figure 2. Schematics of the experimental setup for the readout of the $3 \times 3 \text{ mm}^2$ LySO crystals by the TN3050 JOINBON SiPM.

We aligned the two crystals longitudinally with a plastic support. The distance between the crystal faces was 10 mm. We placed a ^{22}Na point-like β^+ emitter equally spaced between the two crystals, aligned with the center of the crystals.

The signal of the SiPMs was readout without any amplification with the digital oscilloscope (TEKTRONIX DPO71604B) at a sampling frequency of 50 GS/s and with a bandwidth of 1 GHz. The acquisition trigger was formed when the signal crosses a threshold of 4 mV, slightly above the electronics noise fluctuations. The digital waveform was saved within a window of 400 ns starting 80 ns before the trigger time.

2.3 Measurement of the saturation response

As the SiPM has a finite number of cells, its response to a photon flux has a non-linear behavior. We measured a response correction function for each LySO/SiPM detection system used in this experiment. Each LySO crystal was wrapped and coupled to the SiPM as described above.

The crystal was aligned longitudinally with a plastic support. We measured the energy spectrum in response to γ rays with energy 511 keV, 1120 keV, 62.5 keV and 611 keV provided by ^{22}Na , ^{143}Am and ^{137}Cs point-like sources respectively. The readout of the SiPM signals was organized as reported above.

3 Data processing

3.1 Energy resolution

The energy released in the crystal is proportional to the number of photons produced in the scintillation process and thus to the integral of the SiPM signal.

The average voltage of the first 50 ns of the acquired waveform was used for the calculation of the baseline. The baseline-subtracted voltage amplitude of each sample composing the acquired waveform was summed up in a time window ranging between -10 ns and 190 ns with respect to the trigger time. This estimation of the waveform integral E_{sig} was expressed in arbitrary units (A.U.).

According to a first simple linear approximation, the position of the peak corresponding to the photoelectric effect E_{phot} [A.U.] represents the energy E_{γ} [keV] of the γ -ray detected in the LySO

scintillator. Thus a linear calibration of the [A.U.] units into [keV] units is possible by calculating the scale factor $\alpha = E_{\text{gamma}}[\text{keV}]/E_{\text{phot}}[\text{A.U.}]$ and representing the integral of the waveform as $E_{\text{meas}}[\text{keV}] = \alpha E_{\text{sig}}[\text{A.U.}]$.

In order to take into account the non-linear response of the SiPM, we plotted the measured average position of the photoelectric peak $E_{\text{phot}} [\text{A.U.}]$ versus the energy of the detected γ ray. An example is shown in figure 3. We fitted the non-linear response with the function:

$$E_{\text{phot}}[\text{A.U.}] = a (1 - \exp[-bE_{\gamma}[\text{keV}]]) + c \quad (3.1)$$

Thus a non-linear calibration of the [A.U.] units into [keV] physical units is possible by representing the corrected integral of waveform $E_{\text{corr}} [\text{keV}]$ as:

$$E_{\text{corr}}[\text{keV}] = -\frac{1}{b} \log\left(1 - \frac{E_{\text{sig}}[\text{A.U.}] - c}{a}\right) \quad (3.2)$$

We plotted the distribution of $E_{\text{corr}} [\text{keV}]$ and we measured the position $\mu_{\gamma} [\text{keV}]$ and standard deviation $\sigma_{\gamma} [\text{keV}]$ of the photoelectric peak with a gaussian fit. The energy resolution (FWHM) is defined as:

$$\Delta E(\%) = 100 \times 2.35 \times \frac{\sigma_{\gamma}}{\mu_{\gamma}} \quad (3.3)$$

3.2 Coincidence time resolution

We used the data collected in the setup described in section 2.2. The waveforms measured in correspondence of a coincidence detection of a pair of 511 keV photons were analyzed in a time window ranging between -10 ns and 190 ns with respect to the trigger time. We considered only the events where the energy E_{corr} measured in both crystals was within $1 \sigma_{\gamma}$ around the photoelectric peak μ_{γ} .

For both crystals we used a threshold of 5 mV. For each selected event we stored the threshold crossing time of the waveforms of both channels as t_1 [ps] and t_2 [ps]. We analyzed the distribution of the detection time difference $\Delta t = (t_2 - t_1)$ [ps]. We extracted the variance σ_t of the distribution with a gaussian fit. The time resolution (FWHM) was defined as:

$$\Delta t[\text{ps}] = 2.35 \times \sigma_t \quad (3.4)$$

3.3 Multi Voltage Threshold scheme

The aim of the study was to perform a comparison between the energy resolution obtained with a waveform sampled with the high oscilloscope rate and with the MVT threshold technique.

We defined a set of 4 voltage thresholds describing the property of the waveform. As γ -rays undergoing Compton scattering represent a background for the radiation detection applications in consideration, we defined a set of thresholds enhancing the selection performance of the photoelectric events. The lower voltage threshold V_1 was set at 5 mV in order to not perturbate the timing measurement. The highest voltage threshold V_4 was set 5 mV lower than the minimal amplitude of a signal corresponding to the photoelectric photon interaction. The intermediate voltage thresholds $V_{2,3}$ where set at an equal spacing between V_1 and V_4 . The acquired waveforms were represented as a series of 8 voltage levels ($V_1, V_2, V_3, V_4, V_4, V_3, V_2, V_1$) and 8 crossing times ($T_1, T_2, T_3, T_4, T_5, T_6, T_7, T_8$).

The first four samples correspond to the leading edge of the waveform, the second four samples correspond to the falling edge of the waveform.

Following [33], we fitted the 8 points representing the waveform using the function:

$$V(t) = a_1 \times \exp[-a_2 t] \times (1 - \exp[-a_3 t]) \quad (3.5)$$

The integral of the waveform $E^{\text{mvt},i}$ is represented by the analytical integration of eq. (3.5). We assumed a linear relation between $E^{\text{mvt},i}$ and E_{sig} [A.U.] and we calculated a scale factor $\alpha' = E_{\text{sig}}/E^{\text{mvt}}$. The energy in the [A.U.] units is expressed as $E^{\text{mvt},c}$ [A.U.] = $\alpha' E^{\text{mvt},i}$. The corrected energy E^{mvt} [keV], which takes into account the non-linear response of the SiPM, was obtained by applying to $E^{\text{mvt},c}$ [A.U.] the non-linear response function in eq. (3.2).

We plotted the distribution of E^{mvt} [keV] and we measured the position μ_γ^{mvt} [keV] and variance $\sigma_\gamma^{\text{mvt}}$ [keV] of the photoelectric peak with a gaussian fit. The energy resolution (FWHM) is defined as:

$$\Delta E^{\text{mvt}}(\%) = 100 \times 2.35 \times \frac{\sigma_\gamma^{\text{mvt}}}{\mu_\gamma^{\text{mvt}}} \quad (3.6)$$

We performed a comparison between the energy resolution obtained with the MVT approximation ΔE^{mvt} and with the 50 Gsps oscilloscope sampling rate ΔE .

4 Results and discussion

4.1 Energy resolution

The dependence of the average photoelectric signal E_{phot} [A.U.] versus the energy E_γ [keV] of the detected γ -ray is shown on figure 3 for the LySO crystals in both channels and with different lengths. The non-linear response of the LySO/SiPM detection system is fitted with the function in eq. (3.1) and the fitting parameters $a = (162.52 \pm 0.05)$ keV, $b = (1.92 \pm 0.04) \times 10^{-3}$ keV⁻¹, $c = (4.16 \pm 0.11)$ keV are extracted.

The energy spectrum of the two LySO/SiPM detection system in the case of a 10 mm crystal length is shown on figure 3b. The energy with a simple linear scale correction is shown as a red filled histogram and the corrected energy with non-linearity response implementation is shown as the black dots.

The energy resolution (FWHM) at 511 keV estimated for both channels and for the different LySO crystal lengths is shown in figure 4. Within the limits of reproducibility of the experiment in can be approximated with a constant level $\Delta E = (13.50 \pm 0.03)$ %.

The performance of the JOINBON SiPM with respect to the energy resolution is in agreement with the trends reported in the design of PET systems based on SiPM sensors provided by other producers. The typical energy resolution at 511 keV in modern PET systems based on scintillator/SiPM sensing technology ranges in fact between 12% and 14% (FWHM) [6, 7, 36–38]. As expected, the energy resolution does not exhibit any dependence on the crystal length and on the crystal geometry.

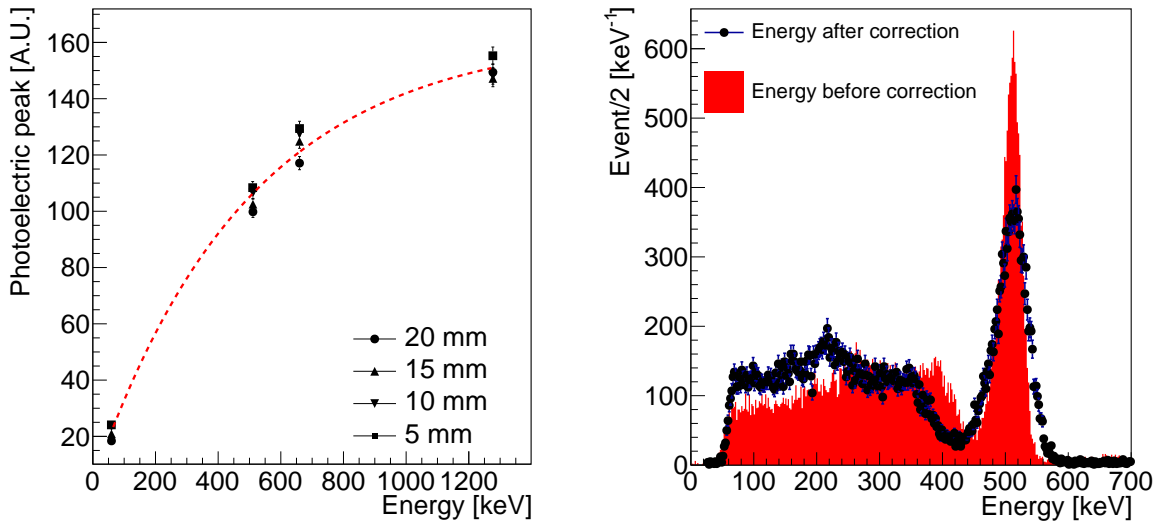


Figure 3. Dependence of the average integrated value (black dots) of the photoelectric signal versus the energy of the detected γ ray for the two crystals (a). The average position of the photoelectric peak is shown for each crystal size. The fitted non linear response correction reported in eq. (3.1) is shown as the red dotted line. The saturation correction is applied to the energy spectrum measured by the LySO/SiPM detection system ($3 \times 3 \text{ mm}^2$) in response to a 511 keV γ ray for the two crystals (b). The photons are detected in coincidence in the two crystals. The spectrum before (filled red histogram) and after (black dots) the saturated response correction is shown.

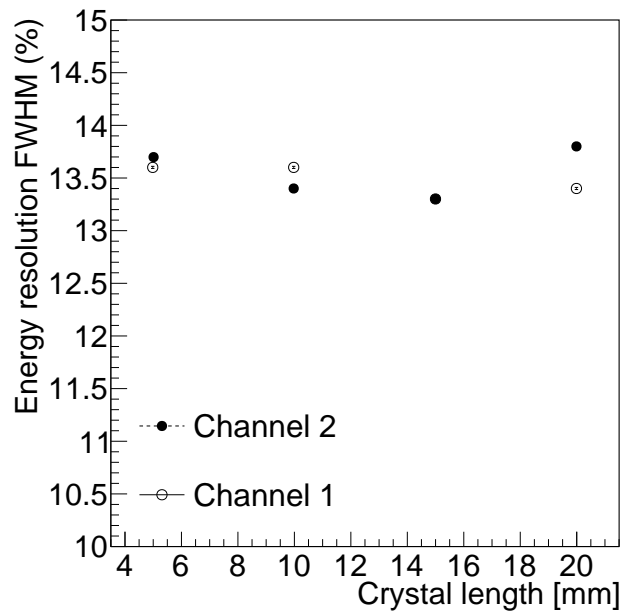


Figure 4. Dependence of the energy resolution at 511 keV (FWHM) on the crystal length, when a pair of 511 keV photons are detected in coincidence in a pair of LySO/SiPM detection systems ($3 \times 3 \text{ mm}^2$).

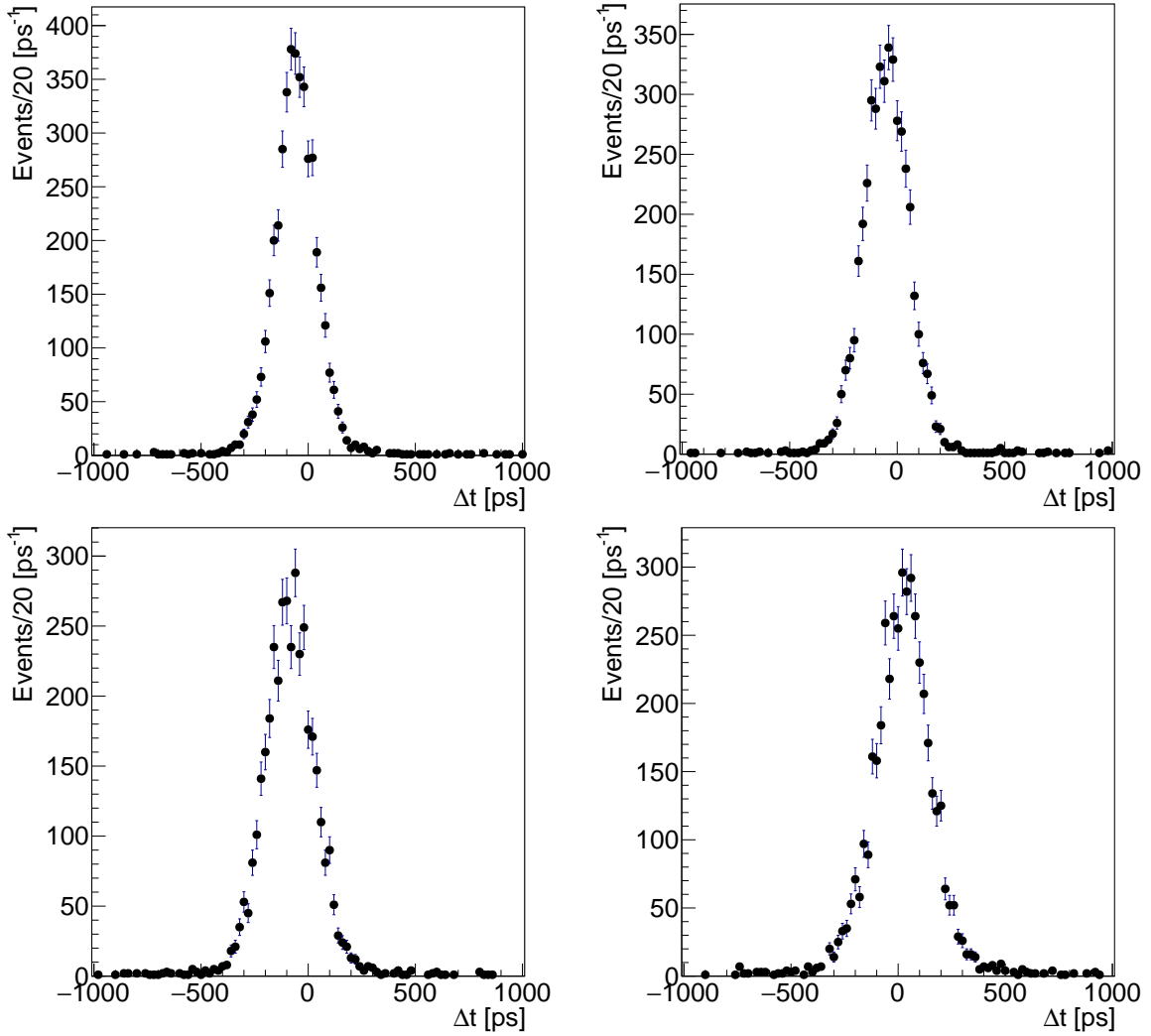


Figure 5. Time difference of two 511 keV photons detected in coincidence and undergoing photoelectric interaction in two LySO/SiPM detection systems ($3 \times 3 \text{ mm}^2$). The crystal length is $5 \times 5 \times 5 \text{ mm}^3$ (a), $5 \times 5 \times 10 \text{ mm}^3$ (b), $5 \times 5 \times 15 \text{ mm}^3$ (c), $5 \times 5 \times 20 \text{ mm}^3$ (d).

4.2 Coincidence time resolution

The time difference of two 511 keV photons detected in coincidence and undergoing photoelectric interaction in two LySO/SiPM detection systems is shown in figure 5 for the different crystal lengths. The measured time resolution (FWHM) is shown as a function of the crystal length in figure 6. It ranges between (215 ± 3) ps for a 5 mm long crystal up to (290 ± 2) ps for a 20 mm long crystal.

The coincidence time resolution is an essential feature for time of flight systems. As reported in [35] dedicated SiPMs for time of flight PET systems reach a single photon time resolution of less than 100 ps, measured in response to a fast pulsed laser. However, the coincidence time resolution of fully engineered systems composed of LySO/SiPM sensors may reach a coincidence time resolution of few hundreds of picoseconds. For instance, the Vereos digital system developed by Philips on the basis of the digital SiPMs (dSiPM) reaches a competitive coincidence time

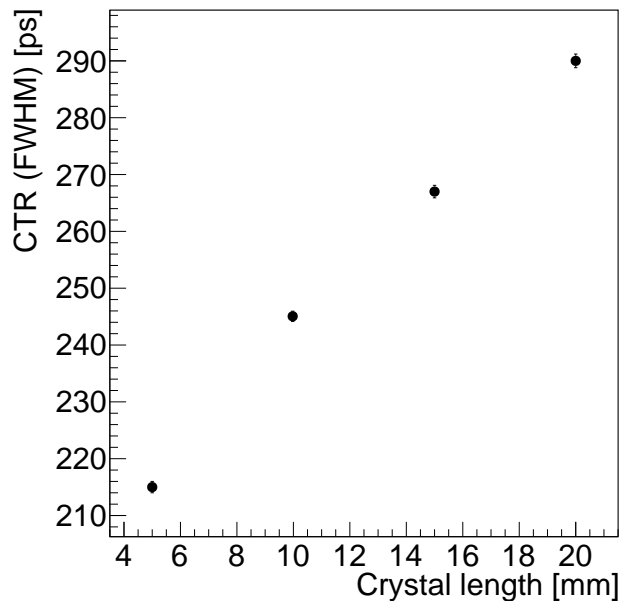


Figure 6. Dependence of the coincidence time resolution (FWHM) on the crystal length, when a pair of 511 keV photons are detected in coincidence and undergo photoelectric interaction in a pair of LySO/SiPM detection systems.

resolution of approximately 300 ps (FWHM) [39]. Thus, the coincidence time resolution of the JOINBON SiPM is in agreement with the expected performances of conventional SiPM devices. The dependence of the coincidence time resolution on the length of the crystals is expected due to the larger number of reflections.

4.3 Multi Voltage Threshold approach

The energy spectrum measured with the by a $3 \times 3 \times 10 \text{ mm}^3$ LySO crystal readout by the TN3050 SiPM in response to a 511 keV γ ray is shown in figure 7. The energy spectrum measured with the 50 Gsps sampling frequency is shown before and after saturation correction as the dotted blue and continuous red histograms.

In the Multi Voltage Threshold approach we represented the waveform using eight samples corresponding to the voltage thresholds $V_i = (5, 30, 55, 80) \text{ mV}$. The energy calculated applying the fitting function (3.5) is shown as the black data points in figure 7. We observe that, as the highest voltage threshold is defined slightly below the minimal amplitude of the photoelectric interaction signals, the MVT sampling method selects only the photoelectric events. The photoelectric peak reconstructed with the MVT method does not show a significant difference from the high sampling frequency method. The energy resolution of the photoelectric peak after non linear response correction is approximately 13.2%.

We have reported a PET prototype for proton therapy monitoring based on LySO/SiPM (SENSL FM30035). The distribution of the energy resolution in the 2880 channels composing the proton therapy monitoring PET prototype with MVT readout shows an average energy resolution (FWHM/phpos) of approximately 24% with a variation (FWHM) of less than 5% across the system [33]. The results presented here demonstrate not only that an optimized selection of the four

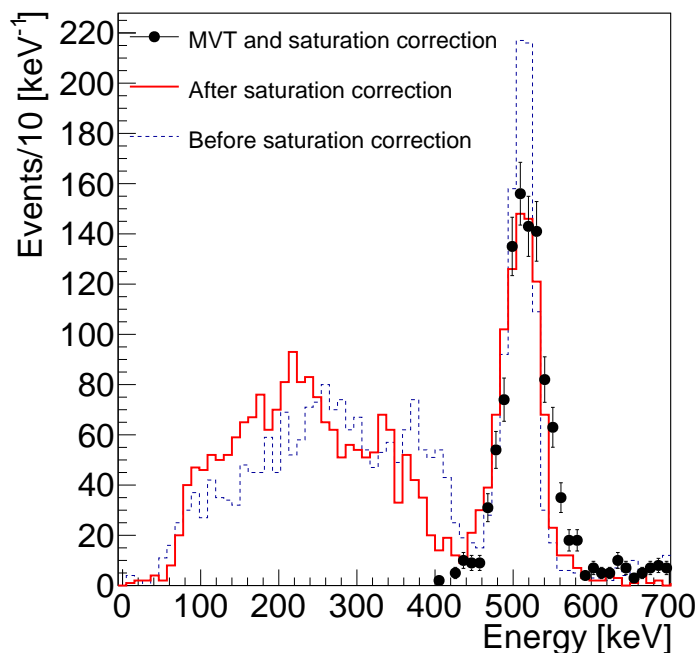


Figure 7. Energy spectrum measured by the LySO/SiPM detection system ($3 \times 3 \text{ mm}^2$) in response to a 511 keV γ ray. The photons are detected in coincidence in the two crystals. The spectrum before (blue dotted line), after (red continuous line) the saturated response correction and with the Multi Voltage Threshold (MVT) method (black filled dots) is shown.

thresholds allow to reach an energy resolution close to the intrinsic detection system capability, but also that the JOINBON SiPM is well suitable to a digital MVT readout.

5 Conclusion

We have presented the performances of the newly released JOINBON SiPMs for potential application to the readout of scintillators. The JOINBON SiPM exhibits an energy resolution of approximately 13.5% and a coincidence time resolution lower than 300 ps (FWHM) for LySO crystal length in the range between 5 mm and 20 mm. The application of a MVT readout scheme allows to reach an energy resolution as low as the intrinsic system characteristics. The properties of the JOINBON SiPMs are ideal for the application to digital Positron Emission Tomography.

Following the promising results of the characterization, the next step of this study will be to realize a full scale prototype of a PET system for brain imaging using the JOINBON SiPM and verify the performances of this new sensor on a larger scale prototype.

Acknowledgments

This work was supported in part by the Natural Science Foundation of China (NSFC) Grant 61671215, in part by National Key Scientific Instrument and Equipment Development Project of China 2016YFF0101500

References

- [1] Ketek PM1150NT, <https://www.ketek.net/> (accessed November 2018).
- [2] SensL C series 10050, <https://www.SensL.com> (accessed November 2018).
- [3] Hamamatsu MPPC S12571-50c, <https://www.hamamatsu.com> (accessed November 2018).
- [4] Excelitas C30742-11-050, <https://www.excelitas.com> (accessed November 2018).
- [5] AdvanSiD ASD-RGB1S-P, <https://www.avansid.com> (accessed November 2018).
- [6] H.J.T. Buitenhuis, F. Diblen, K.W. Brzezinski, S. Brandenburg and P. Dendooven, *Beam-on imaging of short-lived positron emitters during proton therapy*, *Phys. Med. Biol.* **62** (2017) 4654.
- [7] M.A. Piliero et al., *Full-beam performances of a PET detector with synchrotron therapeutic proton beams*, *Phys. Med. Biol.* **61** (2016) N650.
- [8] L. Lestand et al., *In Beam PET Acquisition on 75 MeV. u^{-1} Carbon Beam Using Sampling-Based Read-Out Electronics*, *IEEE Trans. Rad. Plasm. Med. Sci.* **1** (2017) 87.
- [9] S. Helmbrecht et al., *In-beam PET at clinical proton beams with pile-up rejection*, *Z. Med. Phys.* **27** (2017) 202.
- [10] S. Binet et al., *FPGA-based multichannel data acquisition system for prototype in-beam PET*, *Proc. IEEE Nucl. Sci. Symp. Med. Imag. Conf.* (2013) 1.
- [11] S. Ritt, R. Dinapoli and U. Hartmann, *Application of the DRS chip for fast waveform digitizing*, *Nucl. Instrum. Meth. A* **623** (2010) 486.
- [12] B. Joly et al., *An optimal filter based algorithm for PET detectors with digital sampling front-end*, *IEEE Trans. Nucl. Sci.* **57** (2010) 63.
- [13] L.L. Ruckman, G.S. Varner and A. Wong, *The First version Buffered Large Analog Bandwidth (BLABI) ASIC for high luminosity collider and extensive radio neutrino detectors*, *Nucl. Instrum. Meth. A* **591** (2008) 534 [arXiv:0802.2278].
- [14] S. Ritt, *Design and performance of the 6 GHz waveform digitizing chip DRS4*, *Proc. IEEE Nucl. Sci. Symp. Conf. Rec.* (2008) 1512.
- [15] B. Li et al., *Feasibility Study on Silicon Photomultiplier with Epitaxial Quenching Resistors as the Readout for PET Detectors*, *IEEE Trans. Nucl. Sci.* **63** (2016) 17.
- [16] Z. Deng and Q. Xie, *Quadratic Programming Time Pickoff Method for Multivoltage Threshold Digitizer in PET*, *IEEE Trans. Nucl. Sci.* **62** (2015) 805.
- [17] Z. Deng, Q. Xie, Z. Duan and P. Xiao, *Scintillation event energy measurement via a pulse model based iterative deconvolution method*, *Phys. Med. Biol.* **58** (2013) 7815.
- [18] D. Xi, C.-M. Kao, W. Liu, C. Zeng, X. Liu and Q. Xie, *FPGA-only MVT digitizer for TOF PET*, *IEEE Trans. Nuc. Sci.* **60** (2013) 3253.
- [19] X. Wang, Q. Xie, Y. Chen and M. Niu, *Advantages of digitally sampling scintillation pulses in pileup processing in PET*, *IEEE Trans. Nucl. Sci.* **59** (2012) 498.
- [20] D. Xi et al., *Optimization of the SiPM pixel size for a monolithic PET detector*, *Phys. Proc.* **37** (2012) 1497.
- [21] Q. Xie et al., *Potentials of digitally sampling scintillation pulses in timing determination in PET*, *IEEE Trans. Nucl. Sci.* **56** (2009) 2607.

- [22] H. Kim, C.-M. Kao, Q. Xie, H. Frisch, C.-T. Chen and F. Tang, *A multi-threshold method for TOF PET signal processing*, *Nucl. Instrum. Meth. A* **602** (2009) 618.
- [23] Q. Xie, C.-M. Kao, Z. Hsiau, C.-T. Chen, *A new approach for pulse processing in Positron Emission Tomography*, *IEEE Trans. Nucl. Sci.* **52** (2005) 988.
- [24] D. Xi et al., *Modularized compact positron emission tomography detector for rapid system development*, *J. Med. Imag.* **4** (2016) 011006.
- [25] X. Mei et al., *A 72-channel FPGA-only MVT digitizer board and a micro-system for coincidence detection/imaging*, *Proc. IEEE Nucl. Sci. Symp. Med. Imag. Conf.* (2014) 1.
- [26] E. Antonecchia, Q. Chu, A. Di Costanzo, L. Wan, N. D’Ascenzo and Q. Xie, *Simulation study on sensitivity performance of a helmet-shaped brain PET scanner based on Plug&Imaging detector design*, *2020 JINST* **15** C05071.
- [27] X. Liang et al., *NEMA-2008 and In-Vivo animal and plant imaging performance of the large FOV preclinical digital PET/CT system Discoverist 180*, *IEEE Trans. Rad. Plasma Med. Sci.* (2020) 1.
- [28] N. D’Ascenzo et al., *Evaluation of a digital brain Positron Emission Tomography scanner based on the Plug&Imaging sensor technology*, *IEEE Trans. Rad. Plasma Med. Sci.* **4** (2020) 327.
- [29] N. D’Ascenzo et al., *A Novel High Photon Detection Efficiency Silicon Photomultiplier With Shallow Junction in 0.35 μm CMOS*, *IEEE Electron Device Lett.* **40** (2019) 1471.
- [30] X. Liang, N. D’Ascenzo, W. Brockherde, S. Dreiner, A. Schmidt and Q. Xie, *Silicon Photomultiplier with area up to 9 mm² in a 0.35 μm CMOS process*, *IEEE J. Elec. Dev. Soc.* **7** (2019) 239.
- [31] D. Xi et al., *A digital PET system based on SiPMs and FPGA-only MVT digitizers*, *Proc. IEEE Nucl. Sci. Symp. Med. Imag. Conf.* (2014) 1.
- [32] B. Li et al., *A Panel PET With Window: Design Performance Evaluation and Prototype Development*, *IEEE Trans. Rad. Plas. Med. Sci.* **1** (2017) 310.
- [33] N. D’Ascenzo et al., *New digital Plug&Imaging sensor for a proton therapy monitoring system based on positron emission tomography*, *Sensors* **18** (2018) 3006.
- [34] JOINBON JD-3050, <http://www.joinbon.com> (accessed November 2018).
- [35] M.G. Bisogni, A. Del Guerra and N. Belcari, *Medical Applications of Silicon Photomultipliers*, *Nucl. Instrum. Meth. A* **926** (2019) 118.
- [36] S. Muraro et al., *Proton therapy treatment monitoring with the DoPET system: activity range, positron emitters evaluation and comparison with Monte Carlo predictions*, *2017 JINST* **12** C12026.
- [37] L. Brombal et al., *Proton therapy treatment monitoring with in-beam PET: Investigating space and time activity distributions*, *Nucl. Instrum. Meth. A* **861** (2017) 71.
- [38] V. Ferrero, *The INSIDE project: in-beam PET scanner system features and characterization*, *2017 JINST* **12** C03051.
- [39] T. Frach, G. Prescher, C. Degenhardt, R. de Gruyter, A. Schmitzt and R. Ballizany, *The digital silicon photomultiplier — Principle of operation and intrinsic detector performance*, *IEEE Nucl. Sci. Symp. Conf. Rec.* (2009) 1959.